Thermal Degradation and Kinetics of Poly(3-hydroxybutyrate)/Organoclay Nanocomposites

Matko Erceg, Tonka Kovačić, Ivka Klarić*

Summary: Poly(3-hydroxybutyrate)/Cloisite30B (PHB/30B) nanocomposites were prepared by solution-intercalation method. The influence of 30B content on the thermal stability of PHB was investigated. With the addition of 3 wt. % of 30B the highest thermal stability of PHB was achieved. The kinetic analysis of the non-isothermal degradation was performed using the isoconversional Friedman method and invariant kinetic parameters method.

Keywords: kinetics; nanocomposites; non-isothermal thermogravimetry (TG); poly(3-hydroxybutyrate); thermal properties

Introduction

One of the main drawbacks of a fully biodegradable poly(3-hydroxybutyrate) (PHB) is its very low thermal stability at processing temperatures. To improve these properties internal[1,2] and external plasticization[3,4] as well as blending[5,6] of PHB have been performed. In this work, as an alternative to these conventional methods, PHB nanocomposites with organically modified montmorillonite Cloisite30B as a nanofiller, were prepared and their thermal stability determined. Reaction mechanism of the non-isothermal degradation process can be investigated by kinetic analysis. Kinetic parameters, the activation energy (E) and the pre-exponential factor (A) as well as the algebraic expression for reaction mechanism, i.e. kinetic model $f(\alpha)$ were calculated by isoconversional Friedman (FR)[7] method and invariant kinetic parameters (IKP)[8] method.

Experimental Part

Materials

Poly(3-hydroxybutyrate) (PHB), (Biomer, Krailling, Germany; $M_w = 350000$ gmol^{-1}) and organically modified montmorillonite Cloisite30B (30B) (Southern Clay Products Inc., Gonzales, USA; CEC = 90 meq/100 g) were used as received. Cloisite30B is modified with bis-(2-hydroxyethyl)methyl (hydrogenated tallowalkyl) ammonium cations.

Sample Preparation

PHB/30B nanocomposites (100/0, 100/1, 100/3, 100/5, 100/7 and 100/10 by weight) were prepared by the solution-intercalation method. Different amounts of Cloisite30B, depending on sample composition, were dispersed in 50 mL of chloroform by vigorous mechanical stirring for 1 hour and ultra-sonication at 160 W at room temperature for 30 min (pulse mode). In the each obtained dispersion 50 mL of 1% wt/v solution of PHB in chloroform was added and then mixing and ultra-sonication were applied. Mixtures were cast on Petri dishes and the films were obtained by evaporating the solvent at room temperature and drying in vacuum at 40 °C for 24 hours.

Characterization

IR spectroscopy was performed on a Perkin-Elmer Spectrum One FT-IR spectrometer using HATR technique, ZnSe 45 °C crystal, between 650 and 4000 cm^{-1} (resolution of 4 cm^{-1}). The non-isothermal degradation of PHB/30B samples (3.9 ± 0.6 mg) was

Department of Organic Technology, Faculty of Chemistry and Technology, Teslina 10/V, 21 000 Split, Croatia
E-mail: merceg@ktf-split.hr

Copyright © 2008 WILEY-VCH Verlag GmbH & Co. KGaA, Weinheim

performed in the temperature range 50–500 °C at four heating rates (2.5, 5, 10 and 20 °Cmin^{-1}) using a Perkin-Elmer TGS-2 system (the nitrogen flow rate was 30 cm^{3}min^{-1}).

Kinetic Analysis

The kinetic analysis in this work is performed according to algorithm proposed by Budrugeac.[9] It starts with isoconversional method, in this work with FR method. FR method is based on the Eq. (1). E can be obtained from the slope of the linear relationship $ln[\beta d\alpha/dT]$ vs. $1/T$ for $\alpha = \text{const.}$ const. (α is the degree of conversion, β is the heating rate, °Cmin^{-1}). FR method also reveals the dependence of E on α.

$$\ln[d\alpha/dt] \equiv \ln[\beta d\alpha/dT] = \ln[Af(\alpha)] - E/RT \quad (1)$$

If E doesn't depend with α, IKP method and Pérez-Maqueda et. al. criterion[10] can be used for kinetic triplet evaluation (E, A, $f(\alpha)$). IKP method is based on the linear compensation effect between E and lnA (Eq. 2), where a^* and b^* are the compensation effect parameters.

$$\ln A = a^* + b^* E \quad (2)$$

For that purpose, E and lnA are obtained by Coats-Redfern (CR)[11] method (Eq. (3)).

$$\ln g(\alpha)/T^2 \cong \ln AR/\beta E - E/RT \quad (3)$$

where

$$g(\alpha) = \int_0^\alpha d\alpha/f(\alpha)$$

From the slope and intercept of the plots $ln[g(\alpha)/T^2]$ vs. $1/T$ for each theoretical $g(\alpha)$ from Table 1 and each heating rate β, E and lnA can be calculated, respectively. If the compensation effect exists, from the intercept and slope of the straight lines lnA vs. E (Eq. 2) values of a^* and b^* are obtained for each β, respectively. To eliminate the effects of experimental conditions, the invariant kinetic parameters E_{inv} and A_{inv}, are calculated, respectively, from the slope and intercept of the supercorellation relation (Eq. 4).

$$a^* = lnA_{inv} - b^* E_{inv} \quad (4)$$

Values of E_{inv} and A_{inv} allow numerical evaluation of $f_{inv}(\alpha)$ using Eq. (1). The values of $f_{inv}(\alpha)$ are proportional to the true (real) $f(\alpha)$.[9] In order to discriminate the kinetic model, the shape of $f_{inv}(\alpha)$ vs. α curves are compared with the shapes of $f(\alpha)$ vs. α curves corresponding to theoretical kinetic models. Than, the Pérez-Maqueda criterion is applied on the calculated empirical kinetic models which states that only in the case of true kinetic model, all experimental results, at all β, lie on the straight line $ln[\beta(d\alpha/dT)/f(\alpha)]$ vs. $1/T$. From its slope and intercept the true values of E and lnA can be obtained, respectively.

Table 1.
Algebraic expressions for the most frequently used mechanisms.[12]

Mechanism	Symbol	$f(\alpha)$	$g(\alpha)$
Reaction order model	Fn*	$(1-\alpha)^n$	$-\ln(1-\alpha)$, za $n=1$ $(1-(1-\alpha)^{(-n+1)})/(-n+1)$,za $n\neq1$
Random nucleation and growth of nuclei (Avrami-Erofeev eq.)	Am*	$m(1-\alpha)[-\ln(1-\alpha)]^{(1-1/m)}$	$[-\ln(1-\alpha)]^{1/m}$
1D diffusion (parabolic law)	D1	$1/2\alpha$	α^2
1D diffusion (bidimensional particle shape)	D2	$1/[-\ln(1-\alpha)]$	$(1-\alpha)\ln(1-\alpha)+\alpha$
1D diffusion (tridimensional particle shape)	D3	$(3(1-\alpha)^{2/3})/(2[1-(1-\alpha)^{1/3}])$	$[1-(1-\alpha)^{1/3}]^2$
1D diffusion (tridimensional particle shape)	D4	$3/(2[(1-\alpha)^{-1/3}-1])$	$(1-2\alpha/3)-(1-\alpha)^{2/3}$
Power law	Pz*	$z\alpha^{[1-1/z]}$	$\alpha^{1/z}$

*n = 0.5, 2/3, 1.5, 2 and 3; m = 0.5, 1, 1.5, 2, 2.5, 3 and 4; z = 2/3, 2, 3 and 4.

Copyright © 2008 WILEY-VCH Verlag GmbH & Co. KGaA, Weinheim

Results and Discussion

FT-IR spectrograms can be used as an indirect evidence of intercalated structure of PHB/30B nanocomposites. A characteristic change of peak intensity at 840 and 827 cm^{-1}, which correspond to the CH_3 bending in PHB, could explain the nanoscale incorporation of PHB chains with layered silicates.[13] If the PHB chains are intercalated between the silicate layers, layers should restrict the bending and lead to decrease in peak intensities at mentioned wave numbers. The results (Figure 1) show that addition of 30B decreases peak intensities at 839 and 826 cm^{-1} as a consequence of formation of intercalated structure.

In order to establish the influence of 30B content on the thermal stability of PHB, the onset degradation temperatures (T°) (the intersection of the extrapolated base lines with tangents drawn in the inflection of DTG curves) and the temperatures at the maximum degradation rate (T_{max}) (corresponds to the minimum of DTG curves) were determined from non-isothermal thermogravimetry. The results at $\beta = 10\,^{\circ}Cmin^{-1}$ shown in Table 2.

T° and T_{max} of PHB/30B 100/1, 100/3, 100/5 and 100/7 are higher compared to pure PHB and therefore their thermal stability is improved. The highest values of T° and T_{max} are observed for the sample PHB/30B 100/3. The sample PHB/30B 100/10 shows lower values of T° and T_{max} compared to pure PHB, probably due to agglomeration of 30B particles. The influence of 30B content on the T° and T_{max} of PHB is the same at other heating rates. Layered silicates can enhance the thermal stability of polymer by acting as thermal insulator and mass transport barrier against oxygen or volatile degradation products generated during decomposition[14,15], but only if silicates are well dispersed in polymer matrix and in amounts below which agglomeration occurs.

Table 2.
Values of T° and T_{max} at $\beta = 10\,^{\circ}Cmin^{-1}$ for PHB and PHB/30B nanocomposites.

PHB/30B	100/0	100/1	100/3	100/5	100/7	100/10
$T^{\circ}/\,^{\circ}C$	268	279	280	278	273	258
$T_{max}/\,^{\circ}C$	282	291	293	290	288	277

The E values of the non-isothermal degradation process obtained by FR method for PHB and all PHB/30B samples are shown in Table 3. E values are practically constant over the conversion range $0.10 \leq \alpha \leq 0.80$. So, from the kinetically point of view this process is simple and can be described by unique kinetic triplet.[16] Furthermore, IKP method can be applied.

Application of IKP method is explained on sample PHB/30B 100/3. Values of E and lnA obtained by CR method (Eq. 3) for PHB/30B 100/3 are shown in Table 4. Using the Eq. 2, the compensation effect between E and lnA is proven since straight lines are obtained (Table 5, $r^2 = 1$) and from their intercepts and slopes a^* and b^* are

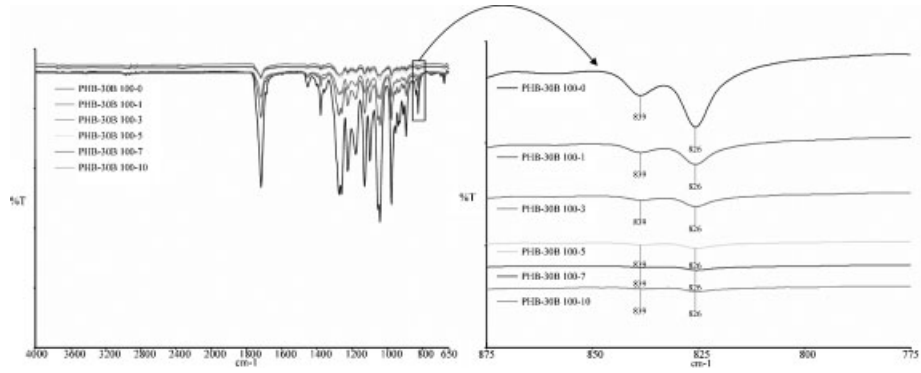

Figure 1.
FT-IR spectrograms of PHB and PHB/30B nanocomposites.

Copyright © 2008 WILEY-VCH Verlag GmbH & Co. KGaA, Weinheim

Table 3.
The average *E* values obtained by FR and IKP methods.

PHB/30B		100/0	100/1	100/3	100/5	100/7	100/10
Conversion, α		$0.10 \leq \alpha \leq 0.80$	$0.10 \leq \alpha \leq 0.80$	$0.10 \leq \alpha \leq 0.80$	$0.10 \leq \alpha \leq 0.80$	$0.10 \leq \alpha \leq 0.80$	$0.40 \leq \alpha \leq 0.80$
FR	E/kJmol^{-1}	139 ± 7	112 ± 6	104 ± 4	103 ± 3	105 ± 2	105 ± 2
	r^2	0.998	0.997	0.998	0.997	0.999	0.994
IKP	E_{inv}/kJmol^{-1}	140	110	103	103	104	105
	ln A_{inv}/min^{-1}	29.9	23.0	21.3	21.2	21.4	21.7
	r^2	1.000	0.997	0.999	0.998	1.000	0.995

Table 4.
Values of *E* and *lnA* obtained by means of CR method for PHB/30B 100/3.

g(α)	$\beta = 2.5$°Cmin^{-1}			$\beta = 5$°Cmin^{-1}			$\beta = 10$°Cmin^{-1}			$\beta = 20$°Cmin^{-1}		
	E/kJmol^{-1}	ln A/min^{-1}	r^2	E/kJmol^{-1}	ln A/min^{-1}	r^2	E/kJmol^{-1}	ln A/min^{-1}	r^2	E/kJmol^{-1}	ln A/min^{-1}	r^2
A0.5	737	165.8	0.999	762	167.5	0.999	722	155.1	0.999	707	148.4	1.000
A1	364	81.1	0.999	376	82.3	0.999	357	76.3	0.999	349	73.3	1.000
A1.5	240	52.7	0.999	248	53.7	0.999	235	49.9	0.999	229	48.1	1.000
A2	178	38.4	0.998	184	39.3	0.999	174	36.6	0.999	170	35.4	1.000
A2.5	140	29.7	0.998	145	30.6	0.999	137	28.6	0.999	134	27.7	1.000
A3	115	23.9	0.998	119	24.8	0.999	113	23.2	0.999	110	22.6	1.000
A4	84	16.6	0.998	87	17.4	0.999	82	16.4	0.999	80	16.1	1.000
F0.5	417	93.4	0.993	431	94.7	0.995	409	87.9	0.994	400	84.3	0.996
F2/3	476	107.1	0.984	492	108.5	0.987	467	100.6	0.986	457	96.6	0.988
F1.5	609	138.1	0.961	631	139.9	0.965	598	129.6	0.965	586	124.3	0.968
F2	561	125.0	0.996	579	126.2	0.994	549	116.9	0.995	537	111.8	0.993
F3	612	136.2	0.999	632	137.6	0.998	599	127.3	0.998	586	121.8	0.997
D1	673	148.8	1.000	695	150.3	1.000	659	139.0	1.000	645	132.9	1.000
D2	632	139.4	1.000	653	140.8	0.999	619	130.2	0.999	606	124.5	0.998
D3	317	70.1	1.000	328	71.2	0.999	310	66.1	0.999	303	63.5	0.999
D4	332	73.6	1.000	343	74.7	1.000	325	69.4	1.000	318	66.6	1.000
P2/3	418	92.8	0.996	432	93.9	0.994	409	87.1	0.994	400	83.4	0.993
P2	134	27.9	0.996	138	28.7	0.994	130	26.8	0.994	127	26.0	0.992
P3	86	16.9	0.995	89	17.6	0.993	84	16.6	0.993	82	16.2	0.992
P4	62	11.2	0.995	64	12.0	0.993	60	11.3	0.993	59	11.2	0.991

calculated, respectively (Table 5). As a^* and b^* are correlated by the supercorrelation relation (Eq. 4) one obtains values of E_{inv} and lnA_{inv} from the slope and intercept of the straight lines (Table 3, $r^2 > 0.99$). Values of E_{inv} and lnA_{inv} allow numerical evaluation of $f_{inv}(\alpha)$ using Eq. (1). Curves $f_{inv}(\alpha)$ vs. α for PHB and all PHB/30B nanocomposites exhibit the maximum (Figure 2(a) is an example for PHB/30B 100/3). From the theoretical ones (Figure 2(b)) only Avrami-Erofeev (*A-E*) kinetic models (A1.5-A4) exhibit maximum. Therefore, non-isothermal degradation of PHB and PHB/30B nanocomposites follows *A-E* kinetic model.

Table 5.
Values of the compensation parameters obtained for PHB/30B 100/3.

β/°Cmin^{-1}	a^*/min^{-1}	b^*/molkJ^{-1}	r^2
2.5	−2.1348	0.2263	1.000
5	−1.4636	0.2202	1.000
10	−0.8860	0.2141	1.000
20	−0.2731	0.2084	1.000

The parameters *m* and *p* of empirical *A-E* kinetic models (shown in Table 6) are calculated from the intercept and slope of plots $ln[(d\alpha/dt)/(1-\alpha)] + lnA + E/RT = lnm + pln[-ln(1-\alpha)]$ obtained by introducing the *A-E* kinetic model into Eq. (1) (if $p = 1-1/m$, empirical kinetic model corresponds to theoretical *Am* kinetic model) for all analysed samples.

Copyright © 2008 WILEY-VCH Verlag GmbH & Co. KGaA, Weinheim

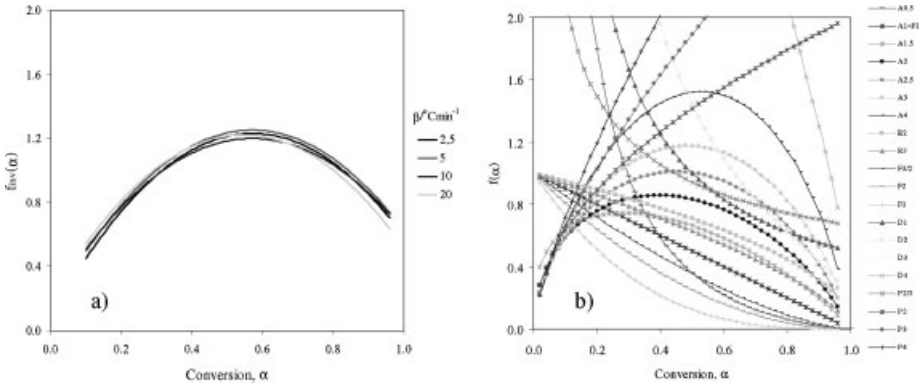

Figure 2.
The experimental (a) and theoretical (b) curves $f(\alpha)$ vs. α for PHB/30B 100/3.

Table 6.
True values of *E* and *lnA* corresponding to the empirical kinetic models $f(\alpha)$.

PHB/25A	Conversion, α	$f(\alpha)$	E/kJmol^{-1}	$ln\ A$/min^{-1}	r^2
100/0	$0.10 \leq \alpha \leq 0.80$	$2.56(1-\alpha)[-\ln(1-\alpha)]^{0.58}$	139	29.7	0.995
100/1	$0.10 \leq \alpha \leq 0.80$	$2.38(1-\alpha)[-\ln(1-\alpha)]^{0.77}$	112	23.5	0.993
100/3	$0.10 \leq \alpha \leq 0.80$	$3.33(1-\alpha)[-\ln(1-\alpha)]^{0.82}$	104	21.3	0.994
100/5	$0.10 \leq \alpha \leq 0.80$	$3.65(1-\alpha)[-\ln(1-\alpha)]^{0.81}$	103	21.2	0.994
100/7	$0.10 \leq \alpha \leq 0.80$	$3.43(1-\alpha)[-\ln(1-\alpha)]^{0.79}$	105	21.5	0.997
100/10	$0.40 \leq \alpha \leq 0.80$	$3.62(1-\alpha)[-\ln(1-\alpha)]^{0.79}$	106	21.9	0.994

The calculated empirical kinetic models fulfil this criterion since straight lines are obtained (Table 6, $r^2 > 0.99$) for pure PHB and all PHB/30B nanocomposites. From their slopes and intercepts the true values of *E* and *lnA* are obtained (Table 6). These *E* values are in a good agreement with the *E* values obtained by FR method (i.e. without any assumption about kinetic model) what proofs the correctness of the kinetic analysis.

Conclusions

PHB/30B nanocomposites were prepared by solution-intercalation method. FT-IR analysis indicate that intercalated nanocomposites were prepared. The addition of Cloisite30B up to 7 wt. % improves the thermal stability of PHB since both T° and T_{max} are shifted toward higher values. The most pronounced effect has the addition of 3 wt. % where T° and T_{max} are higher up to 12 °C. Kinetic analysis of the non-isothermal degradation was performed using isoconversional FR method and IKP method. The true values of kinetic triplets were determined. The non-isothermal degradation of PHB and PHB/30B nanocomposites occurs through a mechanism described by Avrami-Erofeev kinetic model.

[1] V. P. Cyras, A. Vázquez, Ch. Rosza, N. G. Fernández, L. Torre, J. M. Kenny, *J. Appl. Polym. Sci.* **2000**, *77*, 2889.
[2] G. R. Saad, H. Seliger, *Polym. Degrad. Stab.* **2004**, *83*, 101.
[3] E. G. Fernandes, M. Pietrini, E. Chiellini, *Macromol. Symp.* **2004**, *218*, 157.
[4] M. Erceg, T. Kovačić, I. Klarić, *Polym. Degrad. Stab.* **2005**, *90*, 313.
[5] S. N. Lee, M. Y. lee, W. H. Park, *J. Appl. Polym. Sci.* **2002**, *83*, 2945.
[6] S. Godbole, S. Gote, M. Latkar, T. Chakrabarti, *Biores. Biotechnol.* **2003**, *86*, 33.
[7] H. L. Friedman, *J. Polym. Sci.* **1963**, *6C*, 183.
[8] S. V. Vyazovkin, A. I. Lesnikovich, *Thermochim. Acta* **1990**, *165*, 273.
[9] P. Budrugeac, *Polym. Degrad. Stab.* **2005**, *89*, 265.

Copyright © 2008 WILEY-VCH Verlag GmbH & Co. KGaA, Weinheim

[10] L. A. Pérez-Maqueda, J. M. Criado, F. J. Gotor, J. Malek, *J. Phys. Chem. A* **2002**, *106*, 2862.
[11] A. W. Coats, J. P. Redfern, *Nature* **1964**, *201*, 68.
[12] P. Budrugeac, E. Segal, *Int. J. Chem. Kin.* **2001**, *33*, 564.
[13] R. E. Withey, J. N. Hay, *Polymer.* **1999**, *40*, 5147.
[14] B. Han, A. Cheng, G. Ji, S. Wu, J. Shen, *J. Appl. Polym. Sci.* **2004**, *91*, 2536.
[15] C. F. Ou, M. T. Ho, J. R. Lin, *J. Appl. Polym. Sci.* **2004**, *91*, 140.
[16] P. Budrugeac, E. Segal, L. A. Pérez-Maqueda, J. M. Criado, *Polym. Degrad. Stab.* **2004**, *84*, 311.

Copyright © 2008 WILEY-VCH Verlag GmbH & Co. KGaA, Weinheim